

See discussions, stats, and author profiles for this publication at: <https://www.researchgate.net/publication/11458552>

# Synthesis and Biologic Evaluation of a Radioiodinated Quinazolinone Derivative for Enzyme-Mediated Insolubilization Therapy

ARTICLE *in* BIOCONJUGATE CHEMISTRY · MARCH 2002

Impact Factor: 4.51 · DOI: 10.1021/bc010093p · Source: PubMed

CITATIONS

26

READS

24

7 AUTHORS, INCLUDING:



**Bassam A Dahman**

Virginia Commonwealth University

42 PUBLICATIONS 724 CITATIONS

SEE PROFILE



**Kai Chen**

University of Southern California

113 PUBLICATIONS 6,858 CITATIONS

SEE PROFILE



**S. James Adelstein**

Harvard University

113 PUBLICATIONS 2,737 CITATIONS

SEE PROFILE



**Amin I. Kassis**

Harvard Medical School

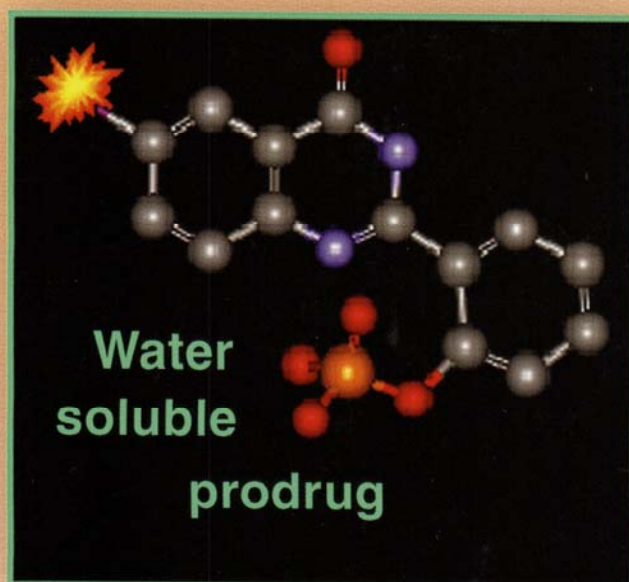
214 PUBLICATIONS 4,118 CITATIONS

SEE PROFILE


# Bioconjugate Chemistry

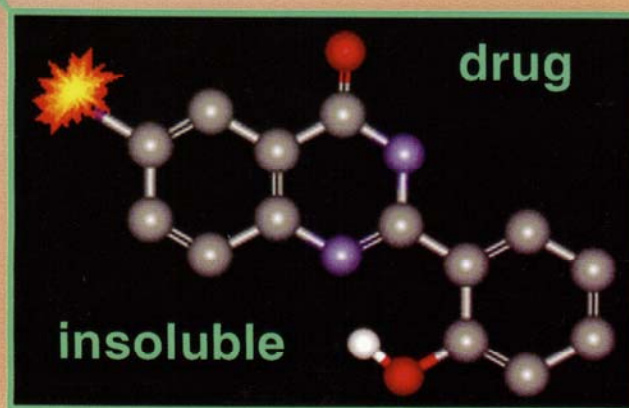
A PUBLICATION OF THE AMERICAN CHEMICAL SOCIETY

March/April 2002  
Volume 13, Number 2  
<http://pubs.acs.org/BC>



Alkaline  
Phosphatase

 :  $^{123}\text{I}/^{124}\text{I}/^{125}\text{I}/^{131}\text{I}/^{211}\text{At}$



# Synthesis and Biologic Evaluation of a Radioiodinated Quinazolinone Derivative for Enzyme-Mediated Insolubilization Therapy

Nan-hui Ho, Ravi S. Harapanhalli, Bassam A. Dahman, Kai Chen, Ketai Wang, S. James Adelstein, and Amin I. Kassir\*

Department of Radiology, Harvard Medical School, Goldenson Building B-242, 220 Longwood Avenue, Boston, Massachusetts 02115. Received October 15, 2001; Revised Manuscript Received January 25, 2002

We have developed a new strategy that aims to concentrate therapeutic radionuclides within solid tumors. This approach, which we have named EMIT (enzyme-mediated insolubilization therapy), is a method for enzyme-dependent, site-specific, *in vivo* precipitation of a radioactive molecule (from a water-soluble precursor) within the extracellular space of solid tumors. The prodrug, ammonium 2-(2'-phosphoryloxyphenyl)-6-iodo-4-(3*H*)-quinazolinone, labeled with iodine-125 ( $^{125}\text{IPD}$ ) and its authentic compound labeled with iodine-127 ( $\text{IPD}$ ) have been synthesized, purified, and characterized. The alkaline phosphatase (ALP)-mediated conversion of these water-soluble nonfluorescent prodrugs to the water-insoluble fluorescent species, iodine-125-labeled 2-(2'-hydroxyphenyl)-6-iodo-4-(3*H*)-quinazolinone ( $^{125}\text{ID}$ ) and its iodine-127-labeled derivative ( $\text{ID}$ ), has been demonstrated *in vitro*. Biodistribution studies in mice indicate that both  $^{125}\text{IPD}$  and  $^{125}\text{ID}$  are minimally retained by most tissues and organs. In addition, following its intravenous injection in mice,  $^{125}\text{IPD}$  is localized in ALP-rich regions and converted to  $^{125}\text{ID}$ , which remains indefinitely within the tissues where it is produced. We believe that EMIT is a strategy that will lead to the active and specific concentration and entrapment of therapeutic radionuclides within solid tumors, the consequent protracted irradiation of tumor cells within the range of the emitted particles, and the effective therapy of solid tumors.

## INTRODUCTION

Monoclonal antibodies (mAb)<sup>1</sup> by virtue of their unique *in vitro* specificity and high affinity for their antigen have been considered particularly attractive as selective carriers of cancer radiotherapeutic atoms/molecules. While most published work on this subject has demonstrated their utility in the diagnosis and treatment of various tumors in *experimental animal models*, the use of radiolabeled mAb to target and treat solid tumors in cancer patients has been for the most part unsuccessful. This failure can be attributed to many causes, including (i) high activity in the whole body, which lowers the maximum tolerated dose (MTD), (ii) limited intratumoral diffusion of the radiolabeled protein molecules and heterogeneity of tumor-associated antigens, both of which lead to nonuniform distribution of the radionuclide within the tumor mass and the consequent sparing of many regions (because either they are outside the range of the emitted particles or they receive a sublethal dose), and (iii) low tumor uptake ( $\sim 0.01\%$  injected dose per gram

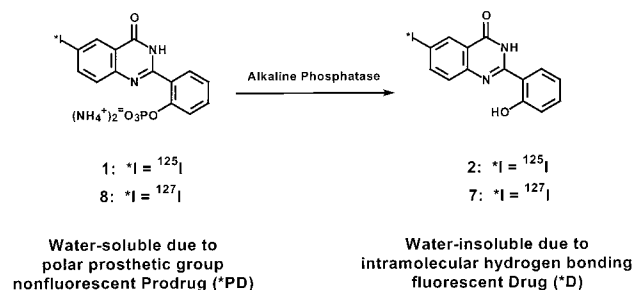
[% ID/g] of tumor in patients versus 5–50% ID/g of tumor in mice). It seems highly probable that the latter point, which is the most distinctive difference between the results obtained from studies in mice and in humans, is the principal factor that has generally led to the therapeutic ineffectiveness of radiolabeled antibodies in man.

In an attempt to bypass some of these limitations, we have been developing a novel strategy that aims to concentrate radioactive molecules within solid tumors. The approach, which we have named EMIT (enzyme-mediated insolubilization therapy), is a method for enzyme-dependent, site-specific, *in vivo* precipitation of a water-soluble radioactive molecule within the extracellular space of solid tumors. In one of its embodiments, the radiolabeled prodrug is hydrolyzed to its water-insoluble form by a constitutive enzyme present in high concentrations within the tumor. In another embodiment, a mAb–enzyme conjugate is injected into tumor-bearing animals. Following its tumor targeting and partial clearance from normal tissues and organs (i.e., high tumor-to-normal-tissue ratios), a water-soluble radioactive substrate to the preadministered enzyme is injected. Owing to the negatively charged prosthetic group(s) present within the substrate, it is highly hydrophilic and consequently not internalized by mammalian cells. On enzymatic hydrolysis, this water-soluble molecule loses its prosthetic group, and the resulting compound is water insoluble and precipitates. The precipitated molecules are concentrated and trapped within the extracellular space of the targeted solid tumor. For EMIT, the substrate may be radiolabeled with an energetic  $\alpha$ - (e.g.,  $^{211}\text{At}$ ,  $^{213}\text{Bi}$ ) or  $\beta$ - (e.g.,  $^{131}\text{I}$ ,  $^{90}\text{Y}$ ) particle-emitting radionuclide. Once precipitated and trapped within the tumor, the prolonged

\* To whom correspondence should be addressed. Telephone: (617) 432-7777. FAX: (617) 432-2419. E-mail: amin\_kassir@hms.harvard.edu.

<sup>1</sup> Abbreviations: mAb, monoclonal antibody; MTD, maximum tolerated dose; %ID/g, percentage injected dose per gram tissue or organ; EMIT, enzyme-mediated insolubilization therapy; ALP, alkaline phosphatase; HPLC, high performance liquid chromatography; THF, tetrahydrofuran; TLC, thin-layer chromatography;  $T_{1/2}$ , half-life; DMSO, dimethyl sulfoxide; ARG, autoradiography; IPD, iodinated prodrug, ammonium 2-(2'-phosphoryloxyphenyl)-6-iodo-4-(3*H*)-quinazolinone; ID, iodinated drug, 2-(2'-hydroxyphenyl)-6-iodo-4-(3*H*)-quinazolinone; ADRT, antibody-directed radioligand targeting; ADEPT, antibody-directed enzyme prodrug therapy; PD, prodrug; D, drug.



**Scheme 1. Conversion of Water-Soluble Prodrug to Water-Insoluble Drug**

residence time should permit delivery of a high radiation dose to the tumor with a low dose to the rest of the body.

In 1994, Haugland et al. (1) described a class of novel substrates made from quinazolinones for the in vitro detection of cell-associated enzyme activity, particularly that of glycosidase, phosphatase, and sulfatase. When the enzyme acts on its weakly fluorescent water-soluble substrate, a highly fluorescent product insoluble in aqueous systems is formed. Using a similar approach, we have synthesized an iodinated ( $^{127}I/^{125}I$ ) derivative of one of these substrates (Schemes 1–3), ammonium 2-(2'-phosphoryloxyphenyl)-6-iodo-4-(3*H*)-quinazolinone (1 and 8). In the presence of alkaline phosphatase (ALP), this water-soluble molecule is hydrolyzed to 2-(2'-hydroxyphenyl)-6-iodo-4-(3*H*)-quinazolinone (2 and 7), a water-insoluble alcohol that precipitates in aqueous solution. We plan to localize such molecules, when labeled with therapeutic radionuclides such as  $^{131}I$  or  $^{211}At$ , within solid tumors that are either innately rich in ALP or that have been pretargeted with an antitumor-antibody-ALP conjugate. We believe that the EMIT approach will lead to the active and specific concentration and entrapment of such therapeutic radionuclides in solid tumors, the consequent protracted irradiation of tumor cells within the range of the emitted particles, and effective therapies of solid tumors. To our knowledge, the use of prodrugs radiolabeled with therapeutic radionuclides has not been reported.

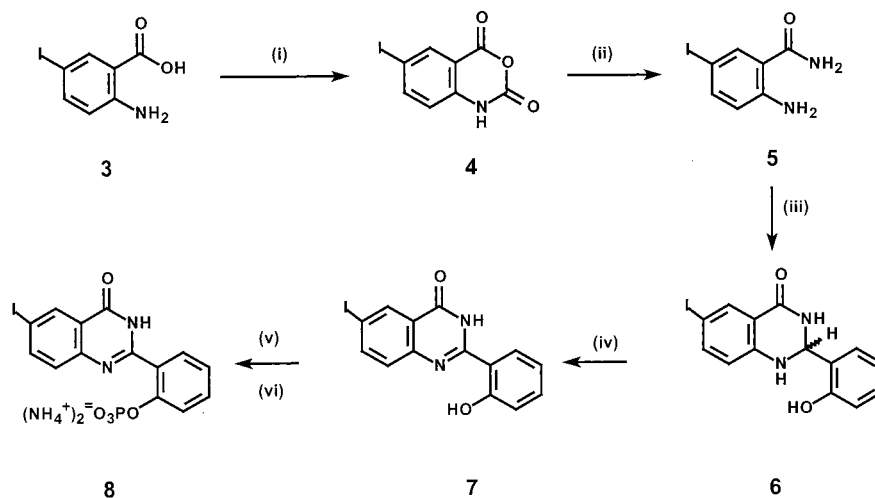
**EXPERIMENTAL PROCEDURES**

**General Remarks.** The reagents were obtained from Sigma Aldrich Chemical Company and used without

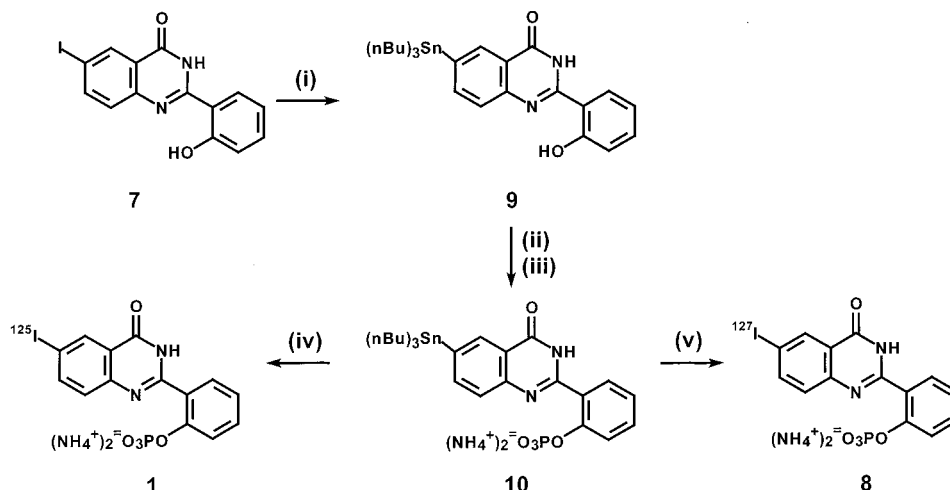
further purification. Carrier-free sodium [ $^{125}I$ ]iodide was obtained from Amersham Corporation. NMR spectroscopy was carried out on either a Varian XL-200 or a Varian XL-500 instrument. Electrospray mass spectra were recorded on a Micromass Platform LCZ mass analyzer. HPLC separations were performed on a reversed-phase Nova-Pak  $C_{18}$  column,  $3.9 \times 30$  mm (Waters Corporation), at a flow rate of 1 mL/min. UV absorption (Waters 486 detector, 286 nm) and  $\gamma$ -ray detection were used to analyze the eluates. High-resolution mass spectrometry was performed on a Bruker Daltonics ApexII 3 T Fourier transform mass spectrometer. Elemental analyses were obtained from Oneida Research Services Incorporated, Oneida, NY.

**Syntheses. Iodoisotoic Anhydride (4).** 2-Amino-5-iodobenzoic acid (3, 2.0 g, 7.6 mmol, Aldrich) and triphosgene (2.26 g, 7.6 mmol) were dissolved in 20 mL of dry THF (freshly distilled from  $CaH_2$ ) (Scheme 2). The reaction mixture was stirred at room temperature for 1 h. An off-white precipitate was formed, and TLC showed that 3 was consumed. The precipitate was filtered and washed with cold methanol. The crude product was redissolved in hot acetonitrile and crystallized (2). After drying in vacuo, 4 was obtained as a white solid (2.0 g, 90%); mp = 235 °C dec.  $^1H$  NMR (DMSO- $d_6$ )  $\delta$  6.94 (d, 1H, ar), 8.01 (d, 1H, ar), 8.11 (s, 1H, ar). ESI-HRMS calcd for  $C_8H_4INO_3-Na$   $[M + Na]^+$ : 311.9128. Found: 311.9126. Anal. Calcd for  $C_8H_4INO_3$ : C, 33.25; H, 1.39; N, 4.85. Found: C, 33.44; H, 1.32; N, 4.90.

**Iodoanthranilamide (5).** A solution of 4 (2.0 g, 6.9 mmol) was suspended in 16 mL of THF. The reaction flask was cooled in an ice-bath. Then 1 mL of 28% aqueous ammonium hydroxide solution was added dropwise to the reaction mixture, accompanied by the evolution of gas. The solution became warm and started to boil. The reaction mixture was stirred for 15 min at 0 °C and 30 min at room temperature. At the end of the reaction, the solution became clear. The solvent was evaporated, and a white solid was obtained. The crude product was filtered to give 5 as a fluffy white solid (1.3 g, 72%).  $^1H$  NMR (DMSO- $d_6$ )  $\delta$  7.80 (s, 1H, ar), 7.37 (d,  $J = 8.5$  Hz, 1H, ar), 7.13 (bs, 2H,  $NH_2$ ), 6.69 (bs, 2H,  $CONH_2$ ), 6.54 (d,  $J = 8.5$  Hz, 1H, ar). ESI-HRMS calcd for  $C_7H_7IN_2O$   $[M + H]^+$ : 262.9676. Found: 262.9674. Anal. Calcd for

**Scheme 2. Pathway for the Synthesis of Ammonium 2-(2'-Phosphoryloxyphenyl)-6-iodo-4(3*H*)-quinazolinone (8) by Method A<sup>a</sup>**

<sup>a</sup> Reagents and conditions: (i) triphosgene/THF; (ii) 28% aqueous ammonium hydroxide/THF; (iii) salicylaldehyde, *p*-toluenesulfonic acid; (iv) 2,3-dichloro-5,6-dicyano-1,4-benzoquinone; (v) phosphorus oxychloride/pyridine/0 °C; (vi) 28% aqueous ammonium hydroxide.

**Scheme 3. Pathway for the Synthesis of Ammonium 2-(2'-Phosphoryloxyphenyl)-6-iodo-4(3*H*)-quinazolinone (1, 8) by Method B<sup>a</sup>**

<sup>a</sup> Reagents and conditions: (i) dioxane/hexa-*n*-butylditin/palladium(0), reflux; (ii) phosphorus oxychloride/pyridine/0 °C; (iii) 28% aqueous ammonium hydroxide; (iv) Na<sup>125</sup>I/iodobeads; (v) Na<sup>127</sup>I/hydrogen peroxide/37 °C.

C<sub>7</sub>H<sub>7</sub>IN<sub>2</sub>O: C, 32.08; H, 2.69; N, 10.69. Found: C, 32.30; H, 2.64; N, 10.78.

2-(2'-Hydroxyphenyl)-6-iodo-2,3-dihydro-4(1*H*)-quinazolinone (**6**). Iodoanthranilamide **5** (1.834 g, 7 mmol) and salicylaldehyde (0.9 mL, 8.4 mmol) were suspended in 25 mL of methanol and refluxed in the presence of catalytic amounts of *p*-toluenesulfonic acid (10%, 0.183 g) for 2 h. After being filtered and washed with cold methanol, **6** was obtained as a pale-yellow solid (2.42 g, 94%). <sup>1</sup>H NMR (DMSO-*d*<sub>6</sub>) δ 9.87 (s, 1H), 8.40 (s, 1H), 8.13 (d, *J* = 8.0 Hz, 1H), 7.82 (s, 1H), 7.50 (t, *J* = 8.75 Hz, 1H), 7.20 (t, *J* = 8.5 Hz, 1H), 6.98 (d, *J* = 7.6 Hz, 1H), 6.82 (d, *J* = 7.6 Hz, 1H), 6.61 (d, *J* = 8.8 Hz, 1H), 5.99 (s, 1H). ESI-HRMS calcd for C<sub>14</sub>H<sub>11</sub>IN<sub>2</sub>O<sub>2</sub> [M + H]<sup>+</sup>: 366.9938. Found 366.9937. Anal. Calcd for C<sub>14</sub>H<sub>11</sub>IN<sub>2</sub>O<sub>2</sub>: C, 45.92; H, 3.03; N, 7.65. Found: C, 46.19; H, 2.74; N, 7.71.

2-(2'-Hydroxyphenyl)-6-iodo-4(3*H*)-quinazolinone (**7**). 2-(2'-Hydroxyphenyl)-6-iodo-2,3-dihydro-4(1*H*)-quinazolinone **6** (1.831 g, 5 mmol) was oxidized by the addition of 2,3-dichloro-5,6-dicyano-1,4-benzoquinone (1.816 g, 8 mmol) in 20 mL of methanol. The suspension was refluxed for 2 h and turned a deep-orange color. After being filtered and washed with cold methanol, the light-yellow solid **7** was obtained (1.52 g, 83.5%). <sup>1</sup>H NMR (DMSO-*d*<sub>6</sub>) δ 11.3 (s, N-H), 8.39 (s, H-7), 8.17 (d, *J* = 8.0 Hz), 8.12 (d, H-5, *J* = 8.75 Hz), 7.56 (d, H-4, *J* = 8.5 Hz), 7.44 (t, H-4', *J* = 7.75 Hz), 6.99 (d, H-6', *J* = 7.5 Hz), 6.95 (t, H-5', *J* = 7.70 Hz). ESI-HRMS calcd for C<sub>14</sub>H<sub>9</sub>IN<sub>2</sub>O<sub>2</sub> [M + H]<sup>+</sup>: 364.9781. Found: 364.9772. Anal. Calcd for C<sub>14</sub>H<sub>9</sub>IN<sub>2</sub>O<sub>2</sub>: C, 46.18; H, 2.49; N, 7.69. Found: C, 45.96; H, 2.46; N, 7.73.

2-(2'-Hydroxy)-6-tributylstannyl-4(3*H*)-quinazolinone (**9**). To a stirred solution of **7** (0.50 g, 1.49 mmol) in 10 mL of dioxane was added hexa-*n*-butylditin (1.89 g, 3.12 mmol) followed by tetrakis(triphenylphosphine)palladium (17.0 mg, 0.015 mmol) as catalyst (Scheme 3). The solution was cloudy and yellow. The reaction mixture was refluxed for 1.5 h, and progress of the reaction was followed by silica gel TLC with methylene chloride:ethyl acetate (9:1) to test for the formation of a more nonpolar product. The solvent was evaporated, and the crude yellow solid was purified on a silica gel column eluted with a stepwise gradient, starting with hexane followed by hexane:dichloromethane (1:1). The solvent was removed to give a yellow fluorescent solid product **9** (0.4 g, 43%). <sup>1</sup>H NMR

(DMSO-*d*<sub>6</sub>) δ 8.24–8.6 (m, 2H, H-7, H-3'), 7.88 (d, H-5, <sup>3</sup>*J* = 7.80 Hz), 7.68 (d, H-4, <sup>3</sup>*J* = 8.10 Hz), 7.43 (t, H-5', <sup>3</sup>*J* = 8.12 Hz), 6.98 (d, H-6', <sup>3</sup>*J* = 9.0 Hz), 6.94 (t, H-4', <sup>3</sup>*J* = 8.0 Hz), 1.51 (quintet, 6H', CH<sub>2</sub>CH<sub>2</sub>Sn, <sup>3</sup>*J* = 7.70 Hz), 1.30 (sextet, 6H', CH<sub>3</sub>CH<sub>2</sub>, <sup>3</sup>*J* = 7.30 Hz), 1.09 (dd, with Sn satellites, <sup>2</sup>*J*<sub>Sn-CH</sub> = 52 Hz, 6H', CH<sub>2</sub>Sn, <sup>3</sup>*J*<sub>avg</sub> = 8.0 Hz), 0.83 (t, 9H', CH<sub>3</sub>CH<sub>2</sub>, <sup>3</sup>*J* = 7.30 Hz). Peak assignment was made using a combination of COSY (2D) and 1D proton NMR spectra. ESI-HRMS calcd for C<sub>26</sub>H<sub>36</sub>N<sub>2</sub>O<sub>2</sub>-Sn [M + H]<sup>+</sup>: 529.1872. Found 529.1878. Anal. Calcd for C<sub>26</sub>H<sub>36</sub>N<sub>2</sub>O<sub>2</sub>Sn: C, 59.23; H, 6.88; N, 5.31. Found: C, 59.48; H, 6.75; N, 5.32.

Ammonium 2-(2'-Phosphoryloxyphenyl)-6-tributylstannyl-4(3*H*)-quinazolinone (**10**). To a stirred solution of **9** (54 mg, 0.108 mmol) in 1 mL of dry pyridine cooled to 0 °C was added dropwise phosphorus oxychloride (20 mg, 0.130 mmol) in 1 mL of dry pyridine. The solution turned yellow. The reaction mixture was stirred for 10 min at 0 °C and then quenched by adding 0.2 mL of 28% ammonium hydroxide solution. The solution was slightly basic (pH 9–10) on pH paper. The reaction mixture after quenching was orange-red. The solvent was evaporated, and a mixture of orange-red-yellow solid was obtained. The crude product was redissolved in methanol:acetate (1:1) and purified on a C<sub>18</sub> column (Waters) using a stepwise gradient, starting with water followed by acetonitrile:water going from 30% to 50% acetonitrile. The solvent was evaporated under reduced pressure (rotary evaporator). An orange-red-yellow nonfluorescent solid (**10**) was obtained (57 mg, 80%). <sup>31</sup>P NMR (DMSO-*d*<sub>6</sub>, H<sub>3</sub>-PO<sub>4</sub> as external reference) δ -17.2. ESI-HRMS calcd for C<sub>26</sub>H<sub>35</sub>N<sub>2</sub>O<sub>5</sub>PSn [M - H]: 605.1228. Found: 605.1226.

Ammonium 2-(2'-Phosphoryloxyphenyl)-6-iodo-4(3*H*)-quinazolinone (**8**). Method A. 2-(2'-Hydroxy)-6-iodo-4(3*H*)-quinazolinone (**7**, 0.1 g, 0.274 mmol) was added to 1 mL of dried pyridine at 0 °C, followed by phosphorus oxychloride (42 mg, 27 μL, 0.274 mmol) dissolved in 0.2 mL of dried pyridine under nitrogen gas (Scheme 2). The reaction was completed within 2 min as indicated by silica gel TLC (chloroform:ethyl acetate:methanol, 3:1:1). The reaction solution became less cloudy and was neutralized to pH 7.0 by adding 0.4 mL (10 mmol) of 28% ammonium hydroxide in 1.5 mL of water at 0 °C. During neutralization, the solution turned orange-red and then light-yellow. At the end of neutralization, the solution

stayed orange-red and some orange-red precipitate was formed. The solvent was evaporated, and a mixture of orange-red and yellow solid was obtained. The solid product was suspended in 2–3 mL of water. The orange-red solid was filtered. The yellow filtrate was purified by chromatography on a 12 cm<sup>3</sup> Sep-Pak Vac C<sub>18</sub> cartridge (Waters) eluted with a stepwise gradient, starting with water (8 mL) followed by acetonitrile:water (2:1, 2 mL). A yellow solution containing UV-visible product was collected. The solvent was evaporated under reduced pressure (rotary evaporator). A yellow nonfluorescent solid (**8**) was obtained (80 mg, 62%). <sup>1</sup>H NMR (DMSO-*d*<sub>6</sub>)  $\delta$  8.36 (d, H-7, <sup>4</sup>*J* = 3.5 Hz), 8.25 (dd, H-3', <sup>3</sup>*J* = 13.5 Hz, <sup>4</sup>*J* = 2.5 Hz), 8.07 (dd, H-5, <sup>3</sup>*J* = 14.3 Hz, <sup>4</sup>*J* = 3.5 Hz), 7.53 (t, H-4', <sup>3</sup>*J* = 13.5 Hz), 7.47 (d, H-4, <sup>3</sup>*J* = 14.5 Hz), 7.22 (t, H-5', <sup>3</sup>*J* = 13.0 Hz), 7.08 (d, H-6', <sup>3</sup>*J* = 13.5 Hz). <sup>31</sup>P NMR (DMSO-*d*<sub>6</sub>, 85% H<sub>3</sub>PO<sub>4</sub> as external reference)  $\delta$  -14.5. ESI-HRMS calcd for C<sub>14</sub>H<sub>8</sub>IN<sub>2</sub>O<sub>5</sub>P [M - H]: 440.9138. Found: 440.9146.

**Method B.** Ammonium 2-(2'-phosphoryloxyphenyl)-6-tributylstannyl-4(3*H*)-quinazolinone (**10**, 15 mg, 0.023 mmol) was dissolved in 0.4 mL of methanol (Scheme 3). Sodium iodide (30 mg, 0.2 mmol) in 0.2 mL of water was added, followed by 0.2 mL of diluted hydrogen peroxide (30% solution diluted 500-fold in water). A yellow precipitate formed immediately. The reaction vial was vortex-mixed and incubated for 15 min at 37 °C. Reversed-phase silica gel TLC (RPSF, Analtech) with acetonitrile:water (1:1) showed approximately 50% conversion. An additional 15-min incubation did not improve the conversion. The solvent was evaporated, and the product was purified by chromatography on a Sep-Pak Plus C<sub>18</sub> cartridge (Waters) eluted with a stepwise gradient, starting with water followed by acetonitrile:water (2:1, 2 mL). A yellow solution containing a UV product was collected, and the solvent was evaporated to yield a yellow nonfluorescent solid. TLC (chloroform:methanol, 1:1) showed the same *R<sub>f</sub>* value (0.6), and proton and <sup>31</sup>P NMR gave the same spectra as were obtained with the known compound **8** synthesized by the other route (Scheme 2). Product **8** was spotted on a TLC plate with alkaline phosphatase and Tris buffer. The TLC plate was incubated for 5 min at 37 °C. After developing the TLC with chloroform, a bright fluorescent spot was seen whose *R<sub>f</sub>* value was the same as that of **7** (*R<sub>f</sub>* = 0.33).

**Preparation of Radiolabeled (<sup>125</sup>I) Ammonium 2-(2'-Phosphoryloxyphenyl)-6-iodo-4(3*H*)-quinazolinone (**1**).** Three iodobeads (Pierce) were placed in a reaction vial, followed by 20  $\mu$ L of **10** (1  $\mu$ g/ $\mu$ L solution) and 30  $\mu$ L of 0.1 M borate buffer (pH = 8.3) (Scheme 3). The desired quantity of Na<sup>125</sup>I (800  $\mu$ Ci, 100  $\mu$ Ci/ $\mu$ L in 0.1 M sodium hydroxide) was added. After 20 min at room temperature, an aliquot was removed for HPLC analysis (the reaction was not quenched with sodium bisulfite since we found that **1** was unstable in reducing reagents). The crude reaction mixture was then loaded on a Sep-Pak Plus C<sub>18</sub> cartridge (Waters) for purification and separation from unreacted organotin precursor (**10**). The column was eluted with 1 mL of water, 2 mL of 10% acetonitrile in water to remove impurities, and finally with 20% acetonitrile in water. The purification was monitored by determining the radioactivity in each tube (Capintec) and analyzing the samples by autoradiography on reversed-phase TLC (acetonitrile:water, 1.5:2). Only the fractions containing a single radioactive spot that had the same *R<sub>f</sub>* as authentic nonradioactive **8** were combined. Approximately 370  $\mu$ Ci of the product (**1**) eluted with the 20% acetonitrile (radiochemical yield, 46%; radiochemical purity, 98%). When **1** was cospotted with nonradioactive

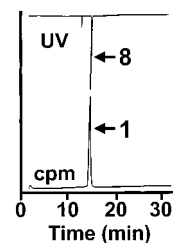


**Figure 1.** HPLC profile of **1** and **8**.

**8** on reversed-phase TLC (acetonitrile:water, 1.5:2), a single spot on autoradiograph was obtained that had the same *R<sub>f</sub>* as **8**. Radiolabeled **1** coinjected with **8** into the HPLC showed a single radioactive peak (*t<sub>R</sub>* = 14 min) that matched the *t<sub>R</sub>* value of **8** (Figure 1).

**Biologic Studies. Enzyme-Dependent Conversion of Prodrug (**8**) to Drug (**7**).** When the water-soluble <sup>127</sup>I-labeled **8** is incubated at 37 °C with alkaline phosphatase (ALP), a clearly visible precipitate is formed whose *R<sub>f</sub>* on TLC corresponds to **7**. To assess the kinetics of this enzyme-based hydrolysis (i.e., conversion of **8** to **7**), **8** (60  $\mu$ M) was mixed with 10 units of ALP in 0.1 M Tris (pH 7.2) containing 50 mM NaCl, 10 mM MgCl<sub>2</sub>, and 0.1 mM ZnCl<sub>2</sub>, and the reaction kinetics were followed over time using a Perkin-Elmer LS50B luminescence spectrometer with excitation at 340 nm and emission at 500 nm. The fluorescence intensity at 500 nm was then plotted as a function of time, the linear portions of the data points were fitted, and the slope was used to calculate the half-life (*T*<sub>1/2 $\alpha$</sub>  and *T*<sub>1/2 $\beta$</sub> ) for the disappearance of **8**.

To assess further the kinetics of this enzyme-based hydrolysis, **8** (2.7  $\mu$ M) was mixed with 40 units of ALP in buffer (pH 9.8), and the reaction kinetics were followed over time. A plot of reciprocal of the substrate (prodrug **8**) concentration (abscissa) versus reciprocal of reaction velocity (ordinate) furnished a straight Lineweaver–Burk line with a slope equal to *K<sub>m</sub>*/*V<sub>max</sub>*; *K<sub>m</sub>* is Michaelis–Menten constant of ALP and *V<sub>max</sub>* is maximum velocity.

**Enzyme-Dependent Conversion of Radioiodinated Prodrug (**1**) to Radioiodinated Drug (**2**).** To characterize the radioiodinated prodrug **1**, 5 units of ALP or heat-inactivated (70 °C, 2 h) ALP were incubated (37 °C) for 3 h with **1** (~10  $\mu$ Ci/100  $\mu$ L of 0.1 M Tris buffer, pH 7.2). Samples were spotted on reversed-phase TLC plates that were then run in acetonitrile:water (1.5:2), and radioactivity was detected by autoradiography.

**Stability of Prodrug **1**.** To assess the chemical nature of the radioactivity in blood post intravenous injection (i.e., determine stability of **1** in blood), mice (*n* = 5) were injected with ~5  $\mu$ Ci of **1** and bled ~40 min later. The samples were pooled, and ethanol was added to precipitate the cells and proteins. Following centrifugation, the supernatant was spotted on TLC, and the plates were run in acetonitrile:water (1.5:2). Autoradiography was used to visualize the radioactivity on the plates.

**Biodistribution of <sup>125</sup>I-Labeled Prodrug (**1**) and Drug (**2**) in Normal Mice.** To determine normal-tissue localization of **1** and **2**, mice (*n* = 5/group) were injected iv or sc with one of the radioiodinated agents and, at 24 h, the animals were killed. The radioactivity associated with blood, heart, lungs, liver, spleen, kidneys, bladder, urine, stomach, small intestine, large intestine, muscles, skin, skeleton, and thyroid was determined in a gamma counter. Based on the injected activity and the weight of these fluids, tissues, and organs, the percentage injected dose per gram (% ID/g) was then calculated.



**Specific Localization of 1 in Alkaline Phosphatase-Rich Regions.** To demonstrate within an animal the conversion of the water-soluble radioiodinated **1** to the water-insoluble **2**, ALP was dissolved in saline (50, 100, 150, 200, 250, 300, 400 units/10  $\mu$ L), and 10  $\mu$ L of the enzyme preparations was injected sc, with a 10- $\mu$ L Hamilton syringe, in the forelimb of Swiss Alpine mice ( $n = 5$ /ALP concentration). Five minutes later, 20  $\mu$ Ci of **1** was injected iv (tail vein). The animals were killed 1 h later, and the radioactivity in the forelimbs was measured. As nonspecific controls, mice ( $n = 5$ ) were injected sc (forelimb) with 200 units of heat-inactivated ALP (56  $^{\circ}$ C, 30 min) prior to the iv injection of **1**.

**Entrapment of 2 within Tissues.** To demonstrate that the water-insoluble ID is retained within the tissue where it is formed, 100  $\mu$ Ci of **7** and 2.5 mg of **2** were added to 100  $\mu$ L of DMSO, and the sample was heated. Under these conditions, the water-insoluble iodinated ( $^{125}\text{I}/^{127}\text{I}$ ) drug dissolves completely, forms a yellow solution, and remains in solution when the sample is cooled to room temperature. However, when 100  $\mu$ L of water is added, a visible precipitate forms immediately. Five microliters of **7**-**2**-DMSO solution was injected sc into the right forelimb of Swiss Alpine mice ( $n = 15$ ) and followed at once by 5  $\mu$ L of saline (the immediate formation of turbidity was noted through the skin of the mice). For comparison, 5  $\mu$ Ci of **1** in 5  $\mu$ L of saline was injected sc into the left forelimb of the same mice and followed immediately with 5  $\mu$ L of DMSO. The animals were killed after 1, 24, and 48 h ( $n = 5$ /time point). The radioactivity associated with the forelimbs was measured, and the percentage of radioactivity remaining at the injection site was calculated.

## RESULTS

**Enzyme-Dependent Conversion of Prodrug (8) to Drug (7).** When nonradiolabeled prodrug **8**, a nonfluorescent, water-soluble compound was incubated with alkaline phosphatase and the kinetics of the hydrolysis were followed with a luminescence spectrometer, a rapid increase in fluorescence intensity (excitation at 340 nm; emission at 500 nm) was observed, demonstrating the hydrolysis of **8** and the formation of **7** (Figure 2, top). Analysis of these data indicates the enzyme-dependent disappearance of **8** (or the appearance of **7**) is biphasic with a  $T_{1/2\alpha}$  of 31 s and a  $T_{1/2\beta}$  of 120 s (Figure 2, bottom). No fluorescence was detected when the enzyme was heat-inactivated prior to its incubation with **8**.

To assess the kinetics of this enzyme-based hydrolysis, the Michaelis-Menten constant of ALP ( $K_m$ ) and maximum velocity ( $V_{max}$ ) were determined by a straight Lineweaver-Burk line with a slope equal to  $K_m/V_{max}$ , where the  $y$  intercept of the line is  $1/V_{max}$  and the  $x$  intercept is  $-1/K_m$ . The calculated  $K_m$  and  $V_{max}$  values, easily determined by extrapolating the straight line to its intercepts on the  $x$  and  $y$  axes, are  $3.07 \times 10^{-6}$  M and  $2.11 \times 10^{-8}$  M/min.

**Enzyme-Dependent Conversion of Radioiodinated Prodrug (1) to Radioiodinated Drug (2).** Reversed-phase TLC followed by autoradiography (ARG) was used to characterize the radiolabeled derivative **1** and confirm its ALP-dependent hydrolysis to **2**. When **1** was cospotted with nonradioactive **8**, a single spot was obtained (ARG) that has the same  $R_f$  as that of **8** (Figure 3). Furthermore, the incubation of **1** with ALP, but not heat-inactivated ALP, led to its complete conversion to **2** (Figure 3). The incubation of **1** with heat-inactivated ALP did not induce any hydrolysis.

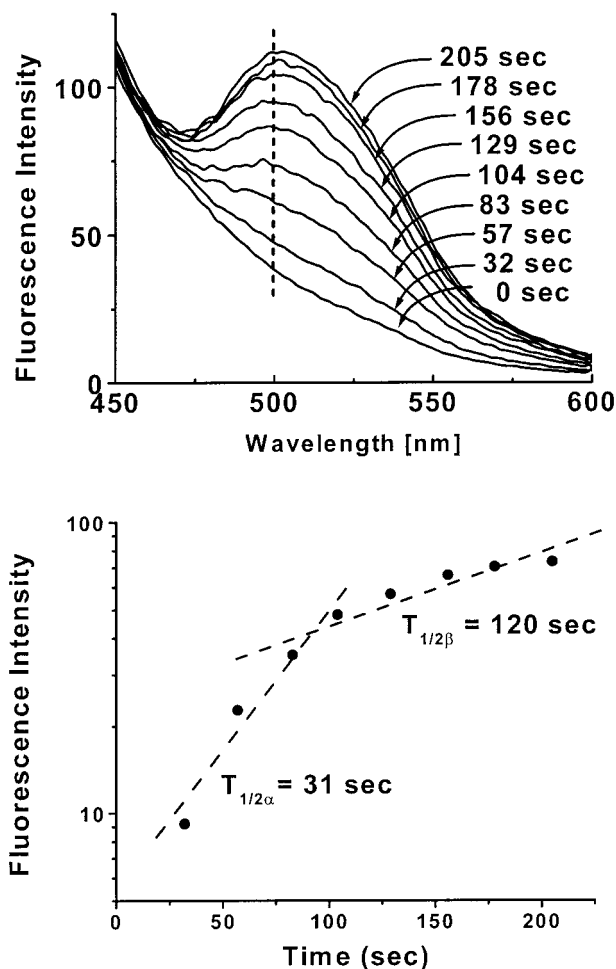


**Figure 2.** Kinetics of alkaline phosphatase-based hydrolysis of **8** to **7** at 37  $^{\circ}$ C. Top: change in fluorescence spectra of **8** as function of time. Bottom: change in fluorescence intensity of **8** at 500 nm as function of time. Linear fits were used to calculate the slopes (data points sets 1–4 and 4–9) and the corresponding  $T_{1/2\alpha}$  and  $T_{1/2\beta}$ .

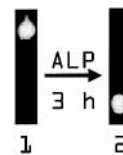


**Figure 3.** Autoradiograph demonstrating complete conversion of **1** to **2** after incubation in alkaline phosphatase at 37  $^{\circ}$ C for 3 h.

**Stability of Prodrug 1.** When the chemical nature of the radioactivity in blood post iv injection in mice was examined, autoradiography demonstrated (i) the presence of a single spot whose  $R_f$  is the same as that of **1**, and (ii) no evidence of free iodide.

**Biodistribution of  $^{125}\text{I}$ -Labeled Prodrug (1) and Drug (2) in Normal Mice.** To assess whether  $^{125}\text{I}$ PD (**1**) and  $^{125}\text{I}$ ID (**2**) are taken up and/or retained by normal tissues, the %ID/g was determined in blood and in various organs and tissues in mice injected iv or sc with  $\sim 5$   $\mu$ Ci of each agent. For  $^{125}\text{I}$ PD (Figure 4, top), the data indicate that (i) similar results were obtained regardless of the injection route, (ii)  $\sim 10\%$  of the injected dose remained in the body of these animals, (iii) some radioactivity was present in the liver (6% ID/g), the kidneys (7% ID/g), and the thyroid (6–12% ID/g), and (iv) minimal amounts of radioactivity ( $< 2\%$  ID/g) were detected in blood and most organs and tissues. These results suggest

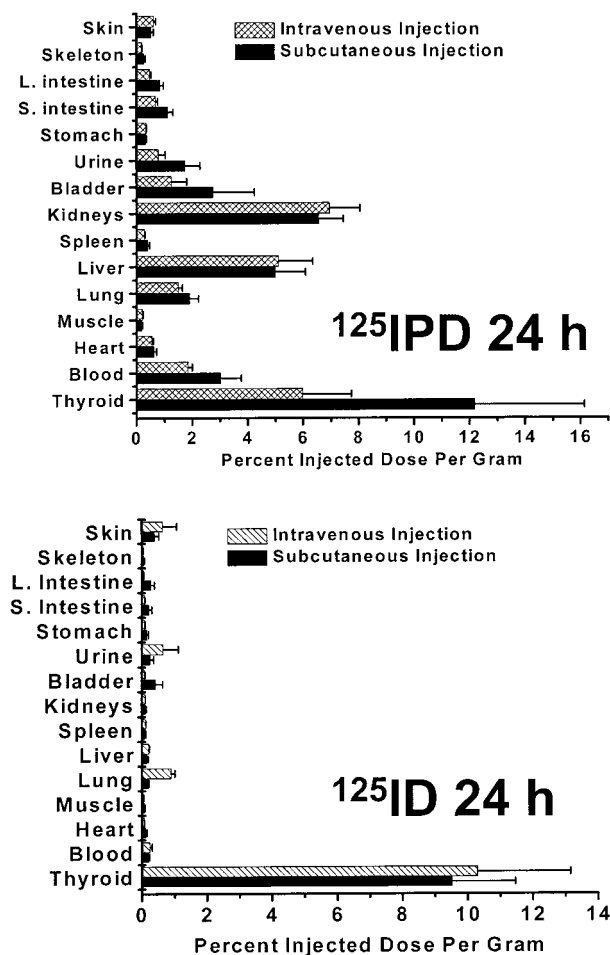


**Figure 4.** Percentage injected dose per gram of tissues, organs, and fluids 24 h post iv or sc injection of compound in normal mice. Top: **1**. Bottom: **2**.

that (i) **1** and/or its breakdown/hydrolysis product(s) are not taken up, hydrolyzed, or retained by most normal tissues and are rapidly excreted through the urinary system, (ii) some dehalogenation of the compound occurs, as exemplified by the presence of activity within the thyroid, and (iii) the accumulation of radioactivity within the liver and kidneys, which are rich in ALP, may be a result of the hydrolysis of **1** and the consequent formation of precipitated **2**. For  $^{125}\text{I}$ D (Figure 4, bottom), minimal radioactivity was observed in all tissues except the thyroid.

**Specific Localization of **1** in Alkaline Phosphatase-Rich Regions.** To demonstrate the hydrolysis of water-soluble **1** to water-insoluble **2** in ALP-rich regions within an animal, mice were injected sc in the forelimb with ALP (or heat-inactivated ALP) and 5 min later iv (tail vein) with 20  $\mu\text{Ci}$  of **1**. The mice were killed 1 h later, and the radioactivity in the forelimb was measured. The data (Figure 5) demonstrate that the radioactive content of the forelimb of animals increased with enzyme dose and plateaued at the highest concentrations. That these increases were due to the enzymatic action of ALP was ascertained in studies that showed no increase in uptake in the forelimb of mice preinjected with heat-inactivated ALP (Figure 5). These results illustrate the specific dose-dependent accumulation of **1** (more accurately **2**) within ALP-containing sites in an animal.

**Entrapment of **2** within Tissues.** To assess the retention of water-insoluble **2** within the tissue where it is formed,  $^{125}\text{I}$ D (**2**) was injected sc into the right forelimb

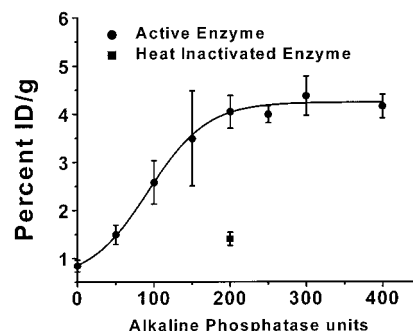


**Figure 5.** Accumulation of radioactivity in forelimbs of mice after sc injection of alkaline phosphatase followed 5 min later by iv injection of **1**.

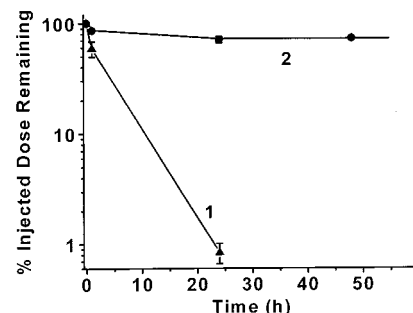


**Figure 6.** Retention of radioactivity in forelimbs of mice after sc injection of **1** and **2**.

of mice (for comparison,  $^{125}\text{I}$ PD (**1**) was injected sc into the left forelimb). The animals were killed at various time periods, and the radioactivity associated with their forelimbs was determined. The data (Figure 6) demonstrate that while  $>99\%$  of prodrug **1** had seeped from the sc pocket by 24 h,  $71 \pm 5\%$  of the injected **2** activity remained at the injection site. As presented earlier (Figure 4, bottom), the radioactivity that escaped from sc injected **2** did not localize in any normal tissues within the animal. Finally, the results show no change in the radioactivity in the forelimbs of the animals ( $\sim 72\%$  injected dose) at 24 and 48 h (Figure 6), indicating that precipitated **2** is permanently and indefinitely trapped within tissues.

## DISCUSSION

The treatment of solid tumors with current therapeutic agents continues to be a problem. Over the past two decades, some investigators have proposed two-step and three-step approaches in which a noninternalizing anti-tumor antibody is injected prior to the administration of a low-molecular-weight therapeutic molecule that has an affinity/reactivity with the preinjected antibody molecule. These systems can be categorized into two major classes: antibody-directed radioligand targeting (ADRT), and antibody-directed enzyme prodrug therapy (ADEPT).

The first strategy (ADRT) is based on the pretargeting of a monoclonal antibody (mAb) moiety that has the capacity to bind simultaneously to tumor cells and a radiotherapeutic molecule. For example, bispecific mAb, in which one valency is directed to a tumor-associated antigen while the other is directed to a radiolabeled molecule, have been preadministered into tumor-bearing animals, and after targeting and clearance of unbound material from the blood pool, the animals are injected with the radiolabeled molecule (3–6). Another system utilizes the high avidity of avidin or streptavidin for biotin ( $k_d = \sim 10^{-15}$  M) to bind the radiolabeled molecule



to the pretargeted antibody (7–10). Both of these systems offer several potential advantages, most prominently (i) rapid blood clearance of the radiopharmaceutical, (ii) short residence of radioactivity in the body, (iii) low radiation doses to normal tissues, and (iv) cross-fire from the emitted long-range particles ( $\alpha$  or  $\beta$ ), negating the need for intracellular localization of the therapeutic agent. A recent report (11) that examined the therapeutic efficacy of a  $^{90}\text{Y}$ -labeled biotin derivative post-pretargeting with an antitumor mAb–avidin conjugate in tumor-bearing mice showed that 100% of the treated animals were cured of their disease, clearly demonstrating the therapeutic potential of such two-step and three-step approaches.

In ADEPT, which was originally described by Philpott in 1973 (12) and later pursued by Bagshawe (13, 14) and Senter (15, 16), a noninternalizing antitumor-antibody–enzyme conjugate is injected into a tumor-bearing animal prior to the administration of a chemotherapeutic agent (prodrug, PD). The enzyme is chosen for its ability to convert the relatively noncytotoxic PD into a highly cytotoxic drug (D). The major advantages offered by ADEPT are (i) low normal tissue toxicity (PD is mildly toxic), (ii) specific conversion of PD in tumors, (iii) high PD-to-D turnover, and (iv) bystander effect (low-molecular-weight D can readily diffuse within the tumor mass and, hence, reach antigen-positive [antibody-targeted] as well as neighboring antigen-negative [antibody nontargeted] tumor cells). However, investigators have realized that, at a minimum, ADEPT has two major limitations: (i) to be therapeutically effective, the cytotoxic agent must be internalized by each cell within the tumor mass (14, 17, 18), and (ii) the toxic agents formed have relatively long biologic half-lives (19) and have been shown to escape from within the tumor mass, thereby increasing nonspecific normal tissue toxicity (14). Despite these shortcomings, various reports have demonstrated that the injection of prodrugs into tumor-bearing animals preinjected with mAb–enzyme conjugates will lead to tumor regression and delay in tumor growth (16, 20). These findings, as well as those reported for ADRT, clearly demonstrate the credibility of such two- and three-step strategies for the treatment of solid tumors.

In this paper, we describe a novel approach, which we have named EMIT (enzyme-mediated insolubilization therapy), that we believe could fulfill many of the basic requirements for the effective therapy of solid tumors. The strategy combines the major advantages of the above-mentioned two approaches while negating their limitations. As mentioned earlier, EMIT is a method for the site-specific, *in vivo* conversion of a water-soluble radioactive molecule (**1**) to a water-insoluble radioactive molecule (**2**) by an enzyme present within a solid tumor. Since many tumors (e.g., prostate, osteosarcomas, teratocarcinomas) have been shown to innately express various phosphatases (21, 22), we expect the hydrolysis of **1** (\*IPD) within the extracellular spaces of such tumors and the indefinite entrapment of the precipitated radioiodinated **2**. Our current data, which demonstrate that  $^{125}\text{I}$ IPD concentrates at sites rich in ALP (Figure 5) and that, once formed, the  $^{125}\text{I}$ ID remains “indefinitely” within the tissue where it is produced (Figure 6), support these expectations. However, for those circumstances where the concentration of the enzyme within a tumor is too low to hydrolyze sufficient amounts of the IPD, the enzyme can be pretargeted to the tumor following its conjugation to a targeting moiety such as a noninternalizing ligand to a tumor-specific receptor or an antitumor antibody, i.e., utilizing the same approaches used in ADEPT. It is

important to note that the EMIT approach bypasses the two main limitations reported for ADEPT since (i) the radiolabeled moiety does not need to be internalized (due to the cross-fire irradiation of cells within the range of the emitted  $\alpha$  and  $\beta$  particles), and (ii) the precipitated molecules formed are trapped within the extracellular spaces of the tumor mass (the biologic half-time within the tumor will in effect equal the physical half-life of the isotope).

For our current studies, we have synthesized (Schemes 2 and 3) a phosporoxyphenol derivative of a radioiodinated quinazolinone (**1**), a water-soluble molecule that is readily hydrolyzed to water-insoluble **2** when exposed to ALP (Scheme 1). While ALP may seem at first inappropriate for EMIT (it is present in most normal mammalian tissues and fluids), our data demonstrate that except for the liver ( $\sim 5\%$  ID/g) and possibly the kidneys ( $\sim 6\%$  ID/g), minimal radioactivity is detected and/or retained in all other normal tissues of mice following the injection of **1** (Figure 4, top). These results indicate that **1** is not taken up, concentrated, or hydrolyzed by most tissues. In addition, the choice of ALP is favored since (i) it is present in high concentration within various tumors (21, 22), (ii) it has a very high second-order rate constant ( $k_{\text{cat}}/K_{\text{M}} = 5 \times 10^7 \text{ M}^{-1} \text{ s}^{-1}$ ), (iii) the availability of its human form should eliminate/reduce its immunogenicity in humans, and (iv) ALP covalently bound to mAb has already been used to activate several chemotherapeutic prodrugs *in vitro* and to retard tumor growth *in vivo* (15, 16, 23–28).

We believe that the approach described in this paper should satisfy most of the requirements for an ideal radiotherapeutic agent, namely (i) rapid and efficient concentration by the tumor, (ii) retention by the tumor (i.e., very long effective clearance half-life), (iii) short residence time within normal tissues (i.e., short effective half-life in blood, bone marrow, and whole body), and (iv) high tumor-to-normal-tissue uptake ratios. Since the PD is labeled with an energetic particle emitter, the therapeutic potential of EMIT will depend on (i) attaining an intratumoral distribution that is sufficiently uniform to match the range of the emitted particles (all tumor cells are within the range of the emitted particles), and (ii) achieving an intratumoral concentration that is sufficiently high to deposit a tumoricidal dose in every cell that is within the range of the emitted particles. Experiments that address these issues are currently ongoing.

## CONCLUSIONS

We have synthesized and characterized  $^{125}\text{I}$ -labeled prodrug (**1**) and its nonradioactive analogue (**8**). The radiochemical yield for no-carrier-added **1** is 46% and the radiochemical purity over 98%. *In vitro*, water-soluble **8** is rapidly and completely converted to a water-insoluble fluorescent precipitate **7** in the presence of alkaline phosphatase. With the exception of the liver, and possibly the kidneys, the radioiodinated prodrug **1** is not taken up/hydrolyzed by normal tissues in mice. However, in ALP-rich regions *in vivo*, it is converted to **2**, which is indefinitely retained within the tissue where it is formed.

We believe EMIT to be a technology that will (i) lead to the active and specific concentration of therapeutic radionuclides within solid tumors, (ii) result in the indefinite entrapment of therapeutic radionuclides within solid tumors, (iii) lead to the protracted irradiation of tumor cells that are within the range of the emitted  $\alpha$  (50–100  $\mu\text{m}$ ) or  $\beta$  (0.1 mm–1 cm) particles, and (iv)

negate the limitations of current prodrug approaches and lead to more effective therapies of solid tumors.

#### ACKNOWLEDGMENT

The authors wish to thank Pulin Wang for his technical assistance.

#### LITERATURE CITED

- (1) Haugland, R. P., Zhang, Y., Yue, S. T., Terpetschnig, E., Olson, N. A., Naleway, J. J., Larison, K. D., and Huang, Z. (1994) Enzymatic analysis using substrates that yield fluorescent precipitates. US Patent 5,316,906.
- (2) Daly, W. H., and Poché, D. (1988) The preparation of N-carboxyanhydrides of  $\alpha$ -amino acids using bis(trichloromethyl)carbonate. *Tetrahedron Lett.* 29, 5859–5862.
- (3) Le Doussal, J.-M., Martin, M., Gautherot, E., Delaage, M., and Barbet, J. (1989) In vitro and in vivo targeting of radiolabeled monovalent and divalent haptens with dual specificity monoclonal antibody conjugates: enhanced divalent hapten affinity for cell-bound antibody conjugate. *J. Nucl. Med.* 30, 1358–1366.
- (4) Le Doussal, J.-M., Gruaz-Guyon, A., Martin, M., Gautherot, E., Delaage, M., and Barbet, J. (1990) Targeting of indium 111-labeled bivalent hapten to human melanoma mediated by bispecific monoclonal antibody conjugates: imaging of tumors hosted in nude mice. *Cancer Res.* 50, 3445–3452.
- (5) Peltier, P., Curtet, C., Chatal, J.-F., Le Doussal, J.-M., Daniel, G., Aillet, G., Gruaz-Guyon, A., Barbet, J., and Delaage, M. (1993) Radioimmunodetection of medullary thyroid cancer using a bispecific anti-CEA/anti-indium-DTPA antibody and an indium-111-labeled DTPA dimer. *J. Nucl. Med.* 34, 1267–1273.
- (6) Bardies, M., Bardet, S., Faivre-Chauvet, A., Peltier, P., Douillard, J.-Y., Mahé, M., Fiche, M., Lisbona, A., Giacalone, F., Meyer, P., Gautherot, E., Rouvier, E., Barbet, J., and Chatal, J.-F. (1996) Bispecific antibody and iodine-131-labeled bivalent hapten dosimetry in patients with medullary thyroid or small-cell lung cancer. *J. Nucl. Med.* 37, 1853–1859.
- (7) Hnatowich, D. J., Virzi, F., and Rusckowski, M. (1987) Investigations of avidin and biotin for imaging applications. *J. Nucl. Med.* 28, 1294–1302.
- (8) Paganelli, G., Riva, P., Deleide, G., Clivio, A., Chiolerio, F., Scassellati, G. A., Malcovati, M., and Siccardi, A. G. (1988) In vivo labelling of biotinylated monoclonal antibodies by radioactive avidin: a strategy to increase tumor radiolocalization. *Int. J. Cancer Suppl.* 2, 121–125.
- (9) Pimm, M. V., Fells, H. F., Perkins, A. C., and Baldwin, R. W. (1988) Iodine-131 and indium-111 labelled avidin and streptavidin for pre-targeted immunoscintigraphy with biotinylated anti-tumour monoclonal antibody. *Nucl. Med. Commun.* 9, 931–941.
- (10) Kassiss, A. I., Jones, P. L., Matalka, K. Z., and Adelstein, S. J. (1996) Antibody-dependent signal amplification in tumor xenografts following pretreatment with biotinylated monoclonal antibody and avidin or streptavidin. *J. Nucl. Med.* 37, 343–352.
- (11) Axworthy, D. B., Reno, J. M., Hylarides, M. D., Mallett, R. W., Theodore, L. J., Gustavson, L. M., Su, F.-M., Hobson, L. J., Beaumier, P. L., and Fritzberg, A. R. (2000) Cure of human carcinoma xenografts by a single dose of pretargeted yttrium-90 with negligible toxicity. *Proc. Natl. Acad. Sci. U.S.A.* 97, 1802–1807.
- (12) Philpott, G. W., Shearer, W. T., Bower, R. J., and Parker, C. W. (1973) Selective cytotoxicity of hapten-substituted cells with an antibody-enzyme conjugate. *J. Immunol.* 111, 921–929.
- (13) Bagshawe, K. D. (1987) Antibody directed enzymes revive anti-cancer prodrugs concept. *Br. J. Cancer* 56, 531–532.
- (14) Bagshawe, K. D. (1994) Antibody-directed enzyme prodrug therapy. *Clin. Pharmacokinet.* 27, 368–376.
- (15) Senter, P. D., Saulnier, M. G., Schreiber, G. J., Hirschberg, D. L., Brown, J. P., Hellström, I., and Hellström, K. E. (1988) Anti-tumor effects of antibody-alkaline phosphatase conjugates in combination with etoposide phosphate. *Proc. Natl. Acad. Sci. U.S.A.* 85, 4842–4846.
- (16) Senter, P. D., Schreiber, G. J., Hirschberg, D. L., Ashe, S. A., Hellström, K. E., and Hellström, I. (1989) Enhancement of the *in vitro* and *in vivo* antitumor activities of phosphorylated mitomycin C and etoposide derivatives by monoclonal antibody-alkaline phosphatase conjugates. *Cancer Res.* 49, 5789–5792.
- (17) Springer, C. J., Antoniow, P., Bagshawe, K. D., and Wilman, D. E. V. (1991) Comparison of half-lives and cytotoxicity of N-chloroethyl-4-amino and N-mesyloxyethyl-benzoyl compounds, products of prodrugs in antibody-directed enzyme prodrug therapy (ADEPT). *Anticancer Drug Des.* 6, 467–479.
- (18) Melton, R. G., and Sherwood, R. F. (1996) Antibody-enzyme conjugates for cancer therapy. *J. Natl. Cancer Inst.* 88, 153–165.
- (19) Antoniow, P., Springer, C. J., Bagshawe, K. D., Searle, F., Melton, R. G., Rogers, G. T., Burke, P. J., and Sherwood, R. F. (1990) Disposition of the prodrug 4-(bis(2-chloroethyl)-amino)benzoyl-L-glutamic acid and its active parent drug in mice. *Br. J. Cancer* 62, 909–914.
- (20) Cheng, T.-L., Chen, B.-M., Chern, J.-W., Wu, M.-F., and Roffler, S. R. (2000) Efficient clearance of poly(ethylene glycol)-modified immunoenzyme with anti-PEG monoclonal antibody for prodrug cancer therapy. *Bioconjugate Chem.* 11, 258–266.
- (21) Herz, F. (1985) Alkaline phosphatase isozymes in cultured human cancer cells. *Experientia* 41, 1357–1361.
- (22) Harris, H. (1989) The human alkaline phosphatases: what we know and what we don't know. *Clin. Chim. Acta* 186, 133–150.
- (23) Sahin, U., Hartmann, F., Senter, P., Pohl, C., Engert, A., Diehl, V., and Pfreundschuh, M. (1990) Specific activation of the prodrug mitomycin phosphate by a bispecific anti-CD30/anti-alkaline phosphatase monoclonal antibody. *Cancer Res.* 50, 6944–6948.
- (24) Senter, P. D. (1990) Activation of prodrugs by antibody-enzyme conjugates: a new approach to cancer therapy. *FASEB J.* 4, 188–193.
- (25) Wallace, P. M., and Senter, P. D. (1991) In vitro and in vivo activities of monoclonal antibody-alkaline phosphatase conjugates in combination with phenol mustard phosphate. *Bioconjugate Chem.* 2, 349–352.
- (26) Haisma, H. J., Boven, E., van Muijen, M., De Vries, R., and Pinedo, H. M. (1992) Analysis of a conjugate between anti-carcinoembryonic antigen monoclonal antibody and alkaline phosphatase for specific activation of the prodrug etoposide phosphate. *Cancer Immunol. Immunother.* 34, 343–348.
- (27) Senter, P. D., Wallace, P. M., Svensson, H. P., Vruthula, V. M., Kerr, D. E., Hellström, I., and Hellström, K. E. (1993) Generation of cytotoxic agents by targeted enzymes. *Bioconjugate Chem.* 4, 3–9.
- (28) Mamber, S. W., Mikkilineni, A. B., Pack, E. J., Rosser, M. P., Wong, H., Ueda, Y., and Forenza, S. (1995) Tubulin polymerization by paclitaxel (taxol) phosphate prodrugs after metabolic activation with alkaline phosphatase. *J. Pharmacol. Exp. Ther.* 274, 877–883.

BC010093P